

Supplementary data

Highly chlorine-oxidation and fouling resistant thin film nanocomposite membrane enhanced by few-layered graphitic carbon nitride nanosheets

Yanan Deng¹, Jianfeng Zhang^{1,3*}, Qingqing Li¹, Tao Liu², Yan Yang³

¹College of Mechanics and Materials, Hohai University, Nanjing 211100, China

²N-Tech Environment Protection Science and Technology (ChangZhou) Co., Ltd. Changzhou
213033, China

³Desalination and Alternative Water Development & Utilization Research Center, Hohai
University, Nanjing 210098, China

*Corresponding author, Email address: jfzhang@hhu.edu.cn, jfzhang_sic@163.com

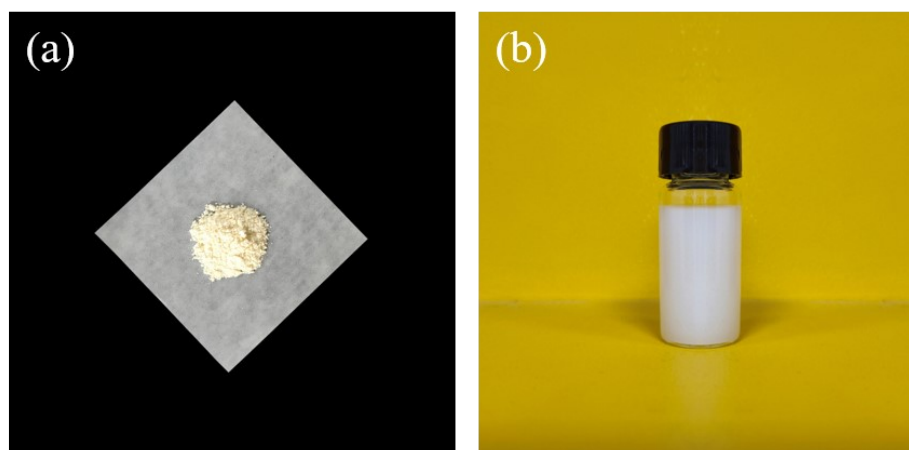


Fig. S1 The powder and dispersion solution images of g-C₃N₄ nanosheets.

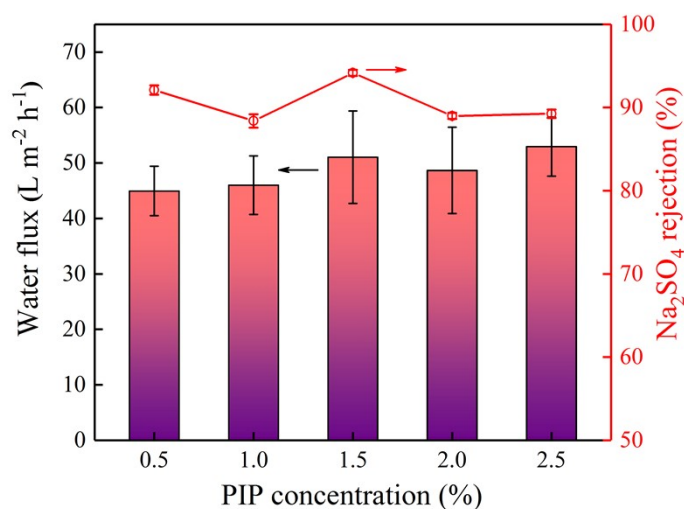


Fig. S2 Water flux and Na₂SO₄ rejection with effects of concentration of PIP. (at 6.0 bar and 2000 ppm Na₂SO₄ salt aqueous solution)

Water flux and Na₂SO₄ rejection with effects of concentration of PIP was shown in Fig. S2. When the concentration of PIP was increased from 0.5 wt% to 1.5 wt%, the Na₂SO₄ rejection increased and reached a maximum value of 94.2% at the concentration of 1.5 wt%. The water flux was observed to increase from 44.9 L m⁻²·h⁻¹ to 51.0 m⁻²·h⁻¹. When the concentration continued to increase, the Na₂SO₄ rejection decreased and remained at about 89.1%, while the water flux also decreased. When the PIP concentration was low, the PA skin layer was loose, and the cross-linking between PIP and TMC was low, which result in the lower Na₂SO₄ rejection. With the increase of PIP, the PA skin layer gradually became denser, and the degree of cross-linking continues to increase. However, when the PIP content was excessive relative to TMC, the IP reaction on the surface was not sufficient and the degree of cross-linking decreased, which led to a significant decrease in the Na₂SO₄ rejection. At the same time, the excess PIP remaining on the surface hindered the channels of water molecules, thus reducing the water flux. Therefore, it was found that the change of water flux was only around 5 L m⁻²·h⁻¹ during the change of PIP, which suggested the effect of PIP concentration was small. At the same time, the effect on the Na₂SO₄ rejection was higher. The performance prepared at a PIP concentration of 1.5 wt% was found to be better considering the higher Na₂SO₄ rejection and water flux. Therefore, the optimal PIP concentration was 1.5 wt%.

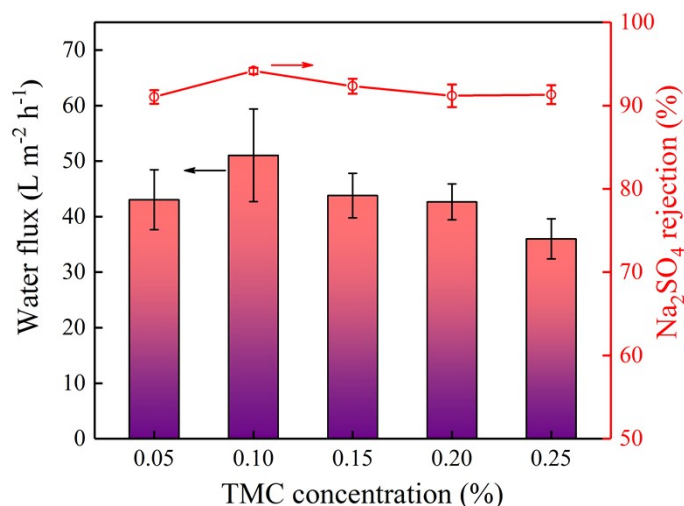


Fig. S3 Water flux and Na₂SO₄ rejection with effects of concentration of TMC. (at 6.0 bar and 2000 ppm Na₂SO₄ salt aqueous solution)

Water flux and Na₂SO₄ rejection with effects of concentration of TMC was shown in Fig. S3. The Na₂SO₄ rejection increased from 91.0% to 94.2% when the content of TMC was increased from 0.05 wt% to 0.10 wt%, and the water flux was observed to increase from 43.0 L m⁻²·h⁻¹ to 51.0 L m⁻²·h⁻¹. With the gradual increase of concentration, the Na₂SO₄ rejection showed a small decrease with a decrease in water flux. When the TMC concentration was low, the PA skin layer on the membrane surface was looser and less cross-linked, while the surface morphology was poorer, resulting in a lower Na₂SO₄ rejection. At the same time, the shrinkage of the PA skin layer was smaller than that of the support layer, which hindered the passage of water molecules and resulted in a lower water flux. With the increase of TMC concentration, the cross-linking of the PA skin layer reached a certain degree, which made the membrane obtain a high Na₂SO₄ rejection. However, when the TMC content was excessive relative to the PIP, the IP reaction was not sufficient and the degree of cross-linking decreased, the Na₂SO₄ rejection decreased significantly. Moreover, the excess TMC on the surface could hinder the passage of water molecules, which reduced the water flux. Considering the results of Na₂SO₄ rejection and water flux, the desalination performance of the membrane prepared at TMC concentration of 0.10 wt% was better. Therefore, the appropriate concentration of TMC was 1.5 wt%.

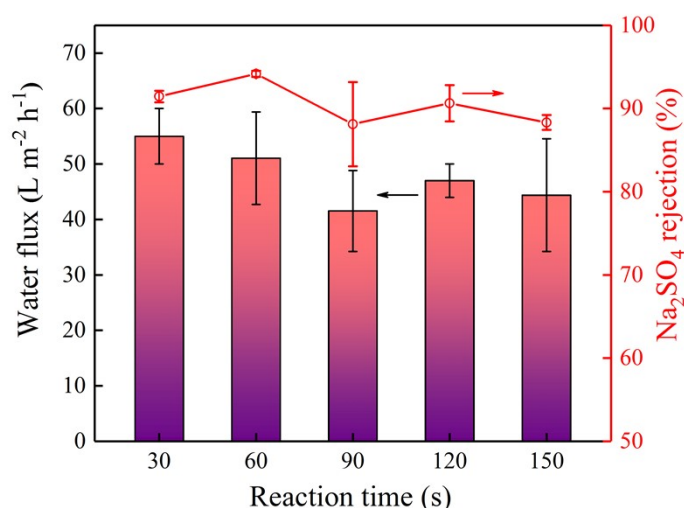


Fig. S4 Water flux and Na₂SO₄ rejection with effects of reaction time. (at 6.0 bar and 2000 ppm Na₂SO₄ salt aqueous solution)

Water flux and Na₂SO₄ rejection with effects of reaction time was shown in Fig. S4. The water flux gradually decreased when the reaction time increased from 30 s to 90 s. The Na₂SO₄ rejection was increased first and then decreased, and reached 94.2% at the reaction time of 60 s. As the reaction time increased, the water flux showed different degrees of decrease, and the Na₂SO₄ rejection decreased to around 88.1%. When the reaction time was extended, the membrane thickness might increase, resulting in a gradual decrease of water flux. In addition, when the reaction time was short, the membranes with suitable crosslinking and thickness were prepared due to the extremely rapid IP reaction. Compared with the membrane prepared at 30 s, the PA skin layer with a reaction time of 60 s was relatively better cross-linked. However, with the increase of reaction time, a barrier could be formed between PIP and TMC, which made the Na₂SO₄ rejection decreased. At the same time, the prolongation of reaction time made part of the TMC inactive and intensify the shrinkage during the heat treatment, which hindered the channels of water molecules. Considering the results of Na₂SO₄ rejection and water flux, the appropriate reaction time is 60 s.

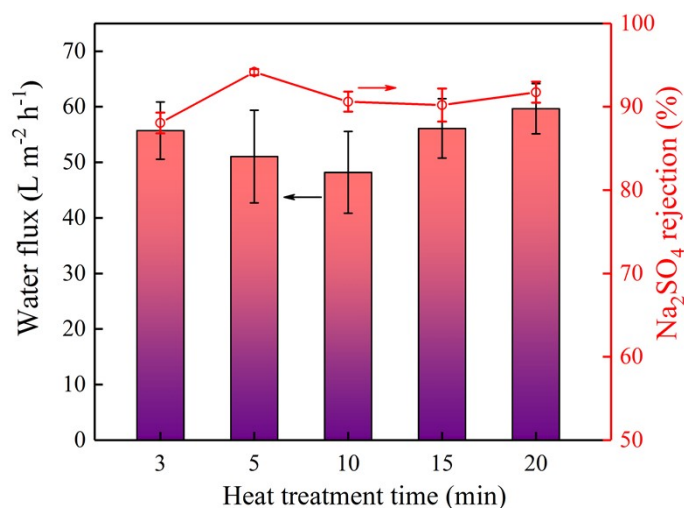


Fig. S5 Water flux and Na_2SO_4 rejection with effects of heat treat time. (at 6.0 bar and 2000 ppm Na_2SO_4 salt aqueous solution)

Water flux and Na_2SO_4 rejection with effects of heat treatment time was shown in Fig. S5. When durations were increased from 3 min to 10 min, the Na_2SO_4 rejection first increased from 88.1% to 94.2%, and then decreased to 90.6%. The water flux was investigated to decrease from $55.7 \text{ L m}^{-2} \text{h}^{-1}$ to $48.2 \text{ L m}^{-2} \text{h}^{-1}$. Subsequently, the Na_2SO_4 rejection stabilized and remained near the level of 90.6% with the increase of reaction time, while the water flux showed an increasing trend. At the short heat treatment time, the cross-linking of PIP with TMC might increase with treatment time, resulting in an increase in the Na_2SO_4 rejection. The subsequent enhancement of the heat treatment time caused the PIP molecules to degrade, which led to a decrease Na_2SO_4 rejection. As the heat treatment time became too long, the surface of the basement membrane underwent a violent shrinkage effect, causing the upper PA skin layer to be destroyed. Considering the results of Na_2SO_4 rejection and water flux, the desalination performance of the membranes was better when the heat treatment time was 5 min, so the optimal heat treatment time was 5 min.

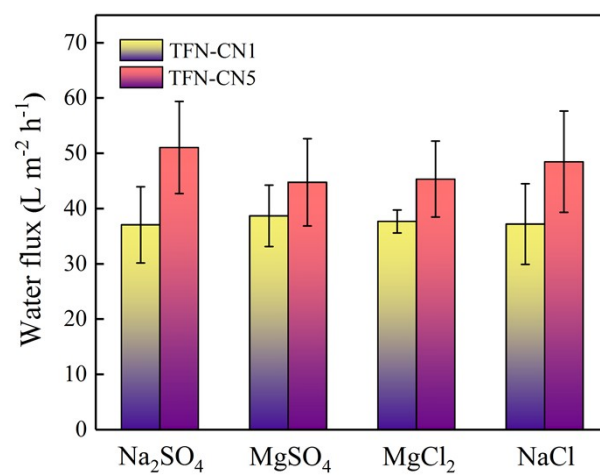


Fig. S6 Water flux of the TFN-CN1 and TFN-CN5 membranes. (at 6.0 bar and 2000 ppm different salt aqueous solution)

Table S1 Elemental compositions of the TFN-CN1 and TFN-CN5 membranes.

Membranes	C (%)	N (%)	O (%)	Cl (%)	O/N
TFN-CN1 before chlorination	81.11	8.57	10.14	0.18	1.18
TFN-CN5 before chlorination	81.71	8.68	9.47	0.14	1.09
TFN-CN1 after chlorination	73.68	11.44	14.30	0.57	1.25
TFN-CN5 after chlorination	75.37	11.19	12.96	0.48	1.15

Table S2 Comparisons of water flux and different salt rejections between the TFN-CN5 membrane and other NF membranes in literature.

Membranes		Pressure (bar)	Concentra tion (ppm)	Water flux (L m ⁻² h ⁻¹)	Na ₂ SO ₄ rejection (%)	MgSO ₄ rejection (%)	MgCl ₂ rejection (%)	NaCl rejection (%)	Ref.
GO	GO TFN (substrate)	8	1000	19.4	95.2	91.1	62.1	59.5	¹
	GO-COCl NF (organic phase)	6	1000	22.6	97.1	>70	–	57.2	²
	SGO TFN (aqueous phase)	5	2500	11.8	96.5	>94.0	–	77.6	³
MoS ₂	MoS ₂ NF (organic phase)	3.5	2000	27.1	94.4	>80	>80	62.7	⁴
	O-MoS ₂ TFN (organic phase)	3.5	2000	27.7	97.9	92.9	86.3	65.1	⁵
	TA-MoS ₂ TFN (aqueous phase)	4.2	1000	31.9	96.5	>85	>25	33.8	⁶
TiO ₂	rGO/TiO ₂ TFN (aqueous phase)	10	2000	61.0	94	–	–	37	⁷
	TA TiO ₂ TFN (aqueous phase)	5	1000	29.0	94.6	96.8	70.5	57.9	⁸
g-C ₃ N ₄	g-C ₃ N ₄ /PA@PSf/PET (aqueous phase)	25	2000	55.7	>70	85.5	>75	>65	⁹
	TFN-CN1	6	2000	37.0	88.5	57.3	17.4	14.4	This work
	TFN-CN5 (aqueous phase)	6	2000	51.0	94.2	74.8	33.6	24.0	This work

References

1. G. S. Lai, W. J. Lau, P. S. Goh, A. F. Ismail, N. Yusof and Y. H. Tan, Graphene oxide incorporated thin film nanocomposite nanofiltration membrane for enhanced salt removal performance, *Desalination*, 2016, **387**, 14-24.
2. P. Wen, Y. B. Chen, X. Y. Hu, B. W. Cheng, D. Q. Liu, Y. F. Zhang and S. Nair, Polyamide thin film composite nanofiltration membrane modified with acyl chlorided graphene oxide, *J. Membr. Sci.*, 2017, **535**, 208-220.
3. Y. Kang, M. Obaid, J. Jang and I. S. Kim, Sulfonated graphene oxide incorporated thin film nanocomposite nanofiltration membrane to enhance permeation and antifouling properties, *Desalination*, 2019, **470**, 12.
4. S. S. Yang and K. S. Zhang, Few-layers MoS₂ nanosheets modified thin film composite nanofiltration membranes with improved separation performance, *J. Membr. Sci.*, 2020, **595**, 11.
5. S. S. Yang, Q. L. Jiang and K. S. Zhang, Few-layers 2D O-MoS₂ TFN nanofiltration membranes for future desalination, *J. Membr. Sci.*, 2020, **604**, 12.
6. H. Zhang, X. Y. Gong, W. X. Li, X. H. Ma, C. Y. Tang and Z. L. Xu, Thin-film nanocomposite membranes containing tannic acid-Fe³⁺ modified MoS₂ nanosheets with enhanced nanofiltration performance, *J. Membr. Sci.*, 2020, **616**, 8.
7. M. Safarpour, V. Vatanpour, A. Khataee and M. Esmaili, Development of a novel high flux and fouling-resistant thin film composite nanofiltration membrane by embedding reduced graphene oxide/TiO₂, *Sep. Purif. Technol.*, 2015, **154**, 96-107.
8. T. Li, Y. R. Xiao, D. X. Guo, L. G. Shen, R. J. Li, Y. Jiao, Y. C. Xu and H. J. Lin, In-situ coating TiO₂ surface by plant-inspired tannic acid for fabrication of thin film nanocomposite nanofiltration membranes toward enhanced separation and antibacterial performance, *J. Colloid Interface Sci.*, 2020, **572**, 114-121.
9. U. Baig, A. Waheed, I. H. Aljundi and R. A. AbuMousa, Facile fabrication of graphitic carbon nitride nanosheets and its integrated polyamide hyper-cross-linked TFC nanofiltration membrane with intrinsic molecular porosity for salts and organic pollutant rejection from water, *J. Mater. Res. Technol.-JMRT*, 2021, **15**, 6319-6328.